


 Cite this: *RSC Adv.*, 2021, **11**, 15656

A sensitive and selective BINOL based ratiometric fluorescence sensor for the detection of cyanide ions†

 Sathishkumar Munusamy, Sathish Swaminathan, Dhanapal Jothi, Vivek Panyam Muralidharan and Sathiyarayanan Kulathu Iyer *

A highly selective, novel BINOL based sensor **BBCN** has been developed for the fluorescent ratiometric detection of cyanide ions (CN^-). The optical study revealed that **BBCN** exhibited unique spectral changes only with cyanide ions in the presence of other competing ions. Besides, an apparent fluorescent colour change from green to blue was observed. A clear linear relationship was observed between the fluorescence ratiometric ratio of **BBCN** and the concentration of CN^- with a reasonably low detection limit (LOD) of 189 nM (507 ppb). The optical response was due to the nucleophilic addition of CN^- to the dicyanovinyl group of the sensor, which compromises the probe's intramolecular charge transfer. This mechanism was well confirmed by Job's plot, $^1\text{H-NMR}$ and ESI-MS studies. **BBCN** showed immediate spectral response towards (1 second) CN^- and detection could be realized in a broad pH window. Furthermore, the practical utility of **BBCN** was studied by test paper-based analysis and the detection of CN^- in various water resources.

Received 14th February 2021

Accepted 20th April 2021

DOI: 10.1039/d1ra01213d

rsc.li/rsc-advances

Introduction

The participation of anions in biological systems and chemical processes is inevitable.^{1–4} Over the past decade, constant effort has been made by the scientific community to understand the fundamental principles of interaction between a host and a negatively charged guest.^{5–13} Though some anions (phosphate, sulphate and carboxylate) are crucial for biological function, cyanide exposure is extremely poisonous to living organisms. The stable complexation of cyanide ion to the active site of cytochrome C has a cascading effect of oxygen transfer inhibition and hypoxiation. Besides, the accumulation of cyanide in the body can lead to cardiac arrest and coma. However, CN^- has widespread application in many fields (electroplating, metallurgy and mining) and cannot be avoided. Hence, the development of a reliable and accurate analytical method is in great demand for various situations. In this regard, development of fluorescent dosimeter for the detection of cyanide ion will be a better choice.^{14–27} Among the fluorescent probes, ratiometric probes have a unique advantage of emission at two different wavelengths providing a built-in correction for environmental effects.^{28–40}

The integral property of fluorescence and chirality of 1,1'-binaphthol (BINOL) and its derivatives have made them

potential candidates for asymmetric catalysis as well as fluorescent chemosensors.^{41–48} Additionally, the fluorescence property and the host-guest interaction of these molecules can be manipulated by adding suitable substitution in the major or minor groove of BINOL. Despite significant reports on the asymmetric synthesis and fluorescent chiral recognition of BINOL, the development of fluorescence sensors involving BINOL for detecting potential small molecules remains very limited. Nevertheless, some BINOL based probes were developed and reported during the last decade. For example, Cheng *et al.*, and Nandhakumar *et al.*, have separately developed BINOL fluorescent derivatives for the selective fluorescent recognition of Hg^{2+} .^{42,49} To detect Al^{3+} , Peng's group linked amino alcohol in the minor groove of BINOL as the reaction site to catch Al^{3+} with turn-on fluorescent responses at low limit of detection (16 ppb).⁵⁰ In 2016, the Yi *et al.*, developed colourimetric and fluorescent off-on sensors for Fe^{3+} based on BINOL-rhodamine derivatives.⁵¹ Besides, quite a few molecular BINOL-derived probes have been designed to sense anions and biologically vital molecules.^{52,53}

In continuation of our research in the development of probes for the molecular recognition^{44–46} in the current article, we report 'turn on' and ratiometric colourimetric, fluorescent probes for cyanide anion, namely, **BBCN**. The synthesized probes have BINOL-dicyanovinyl based platform. BINOL is chosen as the fluorescent core due to its excellent photophysical features and photo stability, whereas, dicyanovinyl group acts as a reaction subunit selective for cyanide ion where it is often employed. Also, the presence of more than one sensing sites in

Department of Chemistry, School of Advanced Sciences, Vellore Institute of Technology, Vellore-632014, India. E-mail: sathiya_kuna@hotmail.com

† Electronic supplementary information (ESI) available. See DOI: 10.1039/d1ra01213d



a probe improve the detection scope. Probe **BBCN** as such exhibits green colour fluorescence and turns into blue-emitting probe over the addition of CN^- . The detailed analytical study revealed that this probe displayed rapid response, highly selective and offered sensitive recognition for tetrabutylammonium cyanide over other competitive anions (F^- , Cl^- , Br^- , I^- , H_2PO_4^- , HSO_4^- , ClO_4^- , and OH^-). The sensing behaviour was analyzed by UV-vis, fluorescence and NMR spectroscopy.

Experimental section

Reagents and equipment

Solvents and reagents were commercially available and procured from commercial sources. Nuclear magnetic resonance spectra were recorded on Bruker Ascent 400 MHz spectrometer. Chemical shift values are reported in δ notation of parts per million using tetramethylsilane (TMS) as the standard. Absorption spectra were recorded on Shimadzu 3600 spectrophotometer while emission spectra were recorded on PerkinElmer LS-55 luminescence spectrometer.

Synthesis and characterization

Synthesis of 1. 6,6'-Dibromo-[1,1'-binaphthalene]-2,2-diol (2.00 g, 6.99 mmol), 4-fluorobenzaldehyde (1.80 mL, 17.1 mmol) and potassium carbonate (2.42 g, 17.5 mmol) were stirred at 100 °C in DMF (50 mL). After 42 h, the reaction mixture was cooled to room temperature, and the target compound was extracted using CH_2Cl_2 . The organic phase was washed with water, dried, and evaporated. The residue was purified by column chromatography over silica gel with CHCl_3 as eluent to give a light-yellow solid.

Synthesis of 2. A mixture of **1** (1 mmol) and malononitrile (2 mmol) was taken in 10 mL of ethanol in a 100 mL conical flask. To the reaction mixture, a catalytic amount of pyridine was added (0.1 mL), and the reaction mixture was stirred at room temperature for about an hour and monitored by TLC. After the completion of the reaction, the reaction mixture was poured into ice-cold water. The formed precipitate was filtered, dried and recrystallized using ethanol and THF solvent composition. The structure of the compound **2** was confirmed by their spectral analysis (^1H NMR and mass spectral analysis). Pale yellow solid; mp-217 °C; ^1H NMR (400 MHz, DMSO-d_6) δ 8.37 (d, J = 5.2 Hz, 4H), 8.17 (d, J = 4.6 Hz, 2H), 7.75 (d, J = 4.2 Hz, 4H), 7.51 (d, J = 4.6 Hz, 4H), 7.10 (d, J = 4.6 Hz, 2H), 6.91 (d, J = 4.2 Hz, 4H) ^{13}C NMR (400 MHz, DMSO-d_6) δ 161.98, 160.56, 150.73, 133.53, 132.57, 132.36, 130.85, 130.78, 127.90, 126.29, 122.45, 121.94, 119.52, 118.13, 114.92, 113.95, 79.04. HRMS for $\text{C}_{40}\text{H}_{20}\text{Br}_2\text{N}_4\text{O}_2$: calculated $[\text{M}^+]$ m/z 745.9953, found 745.9950.

Synthesis of BBCN. To a flame-dried flask, under an argon atmosphere, compound **2** was added and the corresponding terminal alkyne component (3 equiv.), $\text{PdCl}_2(\text{PPh}_3)_2$ (4–6 mol%) and CuI (2–4 mol%) in Et_3N medium were also added. The mixture was heated under reflux for about 4 h. After completing the reaction as indicated by TLC, the mixture was cooled to r.t. The solvent was removed *in vacuo*. Then the residue was dissolved in EtOAc and filtered through a pad of Celite. The

solution was washed with 1 N HCl solution and the aqueous layer was extracted with EtOAc. The combined organic phases were washed with brine, dried over Na_2SO_4 and concentrated *in vacuo*. The resulting crude product was purified by column chromatography (hexane: ethyl acetate, 7 : 3) to afford the pure **BBCN**. The structure of the compound **BBCN** was confirmed by their spectral analysis (^1H NMR and mass spectral analysis). Yellow solid; mp-225 °C; ^1H NMR (400 MHz, DMSO-d_6)TM: δ 6.70 (s, 1H, CH), 7.30 (m, 7H, J = 8.8 Hz, Ar-CH), 7.461 (q, 4H, J = 5.2 Hz, Ar-CH), 7.54 (q, 2H, J = 5.2 Hz, Ar-CH), 7.71 (t, 1H, J = 5.6 Hz, Ar-CH) ^{13}C NMR (DMSO-d_6 , 100 MHz): δ 94.53, 100.04, 115.68, 115.77, 115.89, 115.99, 116.34, 116.55, 118.01, 129.87, 131.11, 132.13, 132.22, 132.56, 132.64, 133.13, 133.37, 140.63, 142.00, 147.15, 161.73, 163.92, 164.17. FT-IR (cm^{-1}): 2249, 1629, 1222, 1053, 1024, 1004, 819, 758, 623. HRMS for $\text{C}_{56}\text{H}_{30}\text{N}_4\text{O}_2$: calculated $[\text{M}^+]$ m/z 790.2369, found 790.2365.

Optical selectivity and titration experiments

Absorption and fluorescence experiments were carried out in 10 mm quartz cuvettes at ambient temperature. For fluorescence measurements, the excitation and emission slit widths were set at 5 nm. The spectral recording was taken immediately after the addition of CN^- as the reaction between CN^- and **BBCN** is rapid. The required quantity of pure **BBCN** was dissolved in acetonitrile solvent (spectroscopic grade) to afford the stock solution (2×10^{-2} M), which was diluted with the solvent medium of $\text{CH}_3\text{CN}/\text{HEPES}$ in water buffer pH 7.2 (7 : 3 v/v) for further studies. Anions were dissolved in deionized water to prepare a stock solution.

Test paper strips of BBCN

BBCN coated filter papers were prepared by dipping the test strips in the solution of (2×10^{-5} M) and then air-dried in an air oven at 40 °C for 30 minutes. Then cyanide and various other anions were tested one by one on **BBCN** coated test papers.

Quantum yield calculation

The quantum yield was calculated using quinine sulfate ($\Phi = 0.54$ in 0.1 M H_2SO_4) as a standard reference using the following formula

$$\Phi_u = \Phi_s \times \frac{F_u}{F_s} \times \frac{A_s}{A_u}$$

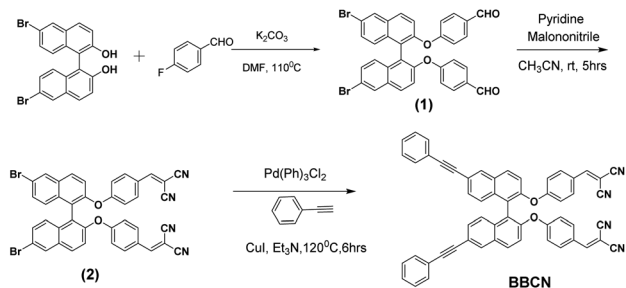
where Φ_s represents the quantum yield, F stands for integrated emission area of corresponding fluorescence spectrum, and A denote absorption intensity of the spectrum. The subscripts 's' and 'u' stand for standard and sample, respectively.

Results and discussion

Design of sensor BBCN

1,1'-Bi-2-naphthol is a stable fluorophore with conformational stability. Its fluorescence property can be modified by introducing suitable substitution at minor groove (3, 3' position) or phenolic -OH group. In this contribution, BINOL based cyanide sensing was designed and synthesized. The synthetic route and





Scheme 1 The stepwise synthetic procedure of BBCN.

molecular structure of sensor **BBCN** are given in Scheme 1. Compound **BBCN** was achieved in three steps by Sonogashira coupling and Knoevenagel condensation.

The probe structure consisted of dicyanovinyl as signalling unit for selective sensing of cyanide ion, and the major groove was incorporated with π extension unit to enhance the optical property. Compound **BBCN** was attained in good yield, which was confirmed by $^1\text{H-NMR}$, $^{13}\text{C-NMR}$, FT-IR, HRMS and HPLC analysis (see ESI; Fig S1–S6†). Probe **BBCN** is soluble in common polar organic solvents such as CH_2Cl_2 , THF, MeOH, and CH_3CN . In this work, CH_3CN was preferred for further analytical studies due to its water miscibility and low toxicity. Compound **BBCN** has very low solubility in water, but with the 7 : 3 ($\text{CH}_3\text{CN} : \text{H}_2\text{O}$) volume ratio with CH_3CN , complete solubility was achieved, and the same solvent composition was used for the analytical studies.

Optical properties of the probes towards CN^-

Compound **BBCN** was dissolved in a mixture of $\text{CH}_3\text{CN}/\text{HEPES}$ in water (7 : 3 v/v) at pH 7.2. It showed two distinct absorption peaks at around 340 nm and 221 nm. The absorption is mainly originated from $\pi-\pi^*$ electron transition and moderate

intramolecular charge transfer (ICT) process. While excess equivalence of anions such as F^- , Cl^- , Br^- , I^- , H_2PO_4^- , HSO_4^- , ClO_4^- , OH^- , S^{2-} , CO_3^{2-} , AcO^- , SCN^- and N_3^- did not generate any change in the absorption spectral pattern (Fig. 1a), the addition of CN^- to the probe showed significant changes in the absorption spectra. On constant increment of CN^- , the intensity of the peak at around 342 nm decreased remarkably, and the peak at about 222 nm showed an increase in peak intensity **BBCN** (Fig. 1b). Furthermore, the absorption spectra of the probes showed a blue shift with increasing concentration of CN^- . An isosbestic point spot observed at 274 nm was indicative of new product formed between **BBCN** and CN^- . The decrease in absorption intensity value at $A_{342 \text{ nm}}$ of **BBCN** varied linearly as a function of the cyanide concentration and reached plateau almost at 2 equiv. of CN^- . The linearity of the equation was calculated to be $y = -0.0651 + 1.0711x$ with the coefficient of determination R^2 value, which was found to be 0.9965 (Fig. 1c).

Similarly, the fluorescence behaviour of the probe **BBCN** was also studied with and without the addition of CN^- in the solvent medium of $\text{CH}_3\text{CN}/\text{HEPES}$ in water (7 : 3 v/v) buffer at pH 7.2. As shown in Fig. 2a, when the probe **BBCN** is excited at 274 nm, a clear emission peak appeared at the 395 nm ($\Phi = 0.18$), which could be attributed to the emission of BINOL core and the ICT emission, respectively. Upon the addition of 2 equiv. of CN^- ion, the intensity of the emission peak at 395 nm got decreased significantly with the simultaneous appearance of a blue-shifted peak at 315 nm ($\Phi = 0.23$). The intensity of the new peak at 315 nm was found to be 180% higher than the peak at 395 nm. To ascertain the fluorescence selectivity of **BBCN** towards various competitive anions, including highly nucleophilic F^- and SCN^- was tested. As shown in the Fig. 2a, except CN^- other anions had almost no effect on the fluorescence

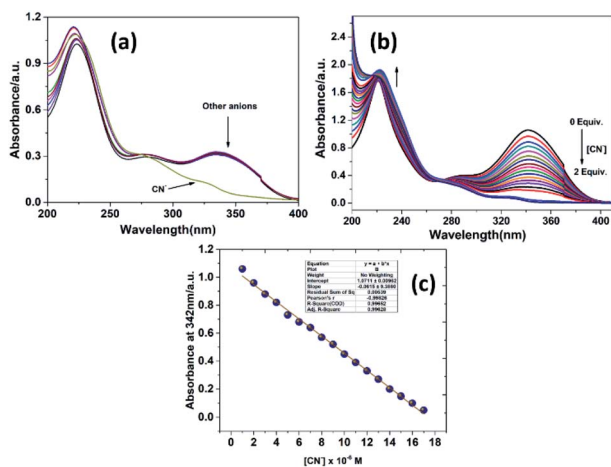


Fig. 1 (a) Absorption spectra of dye **BBCN** (10 μM) in the presence of various anions. (b) Absorption spectra of **BBCN** (10 μM) upon the incremental addition of CN^- in $\text{CH}_3\text{CN}/\text{HEPES}$ in water (7 : 3 v/v) at pH 7.2. CN^- concentrations were varied from 0 to 20 μM . (c) The linear relation for the concentration of CN^- in the range of 0–20 μM .

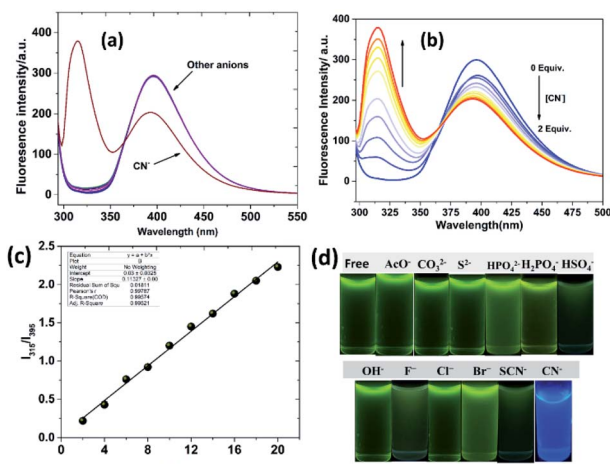


Fig. 2 (a) Fluorescence spectra of dye **BBCN** (10 μM) in the presence of various anions in the solvent medium of $\text{CH}_3\text{CN}/\text{HEPES}$ in water (7 : 3 v/v) at pH 7.2. (b) Fluorescence spectra of **BBCN** (10 μM) upon the incremental addition of CN^- in $\text{CH}_3\text{CN}/\text{HEPES}$ in water (7 : 3 v/v) at pH 7.2. CN^- concentrations were varied from 0 to 20 μM . (c) The linear relation of I_{315}/I_{395} for the concentration of CN^- in the range of 0–20 μM . (d) Fluorescence colour change of **BBCN** over the addition of various anions when viewed under the UV lamp.



behaviour of **BBCN**. This selectivity is indicated in the bar plot in Fig. S7,† which represents the change in fluorescence ratio (I_{315}/I_{395}) in the presence of various anions.

To study the quantitative detection of CN^- , fluorescence titration experiment of probe **BBCN** (20 μM) over the incremental addition of CN^- (0–40 μM) was carried out as shown in Fig. 2b. As can be seen, the intensity of fluorescence peak at 395 nm decreased, while a new emission peak at 315 nm emerged and increased gradually with increasing concentration of CN^- . Notably, an isoemission point at 365 nm was observed, which indicates a straightforward reaction process between CN^- and **BBCN**. The plot of fluorescence intensity ratio (I_{315}/I_{395}) against the concentration of CN^- was found to be linear with the coefficient of determination R^2 value of 0.9957, which indicated the determination of CN^- concentration ratiometrically (Fig. 2c). Limit of detection (LOD) is the most critical attribute of an exemplary sensor. LOD of **BBCN** was calculated based on the fluorescence titration method using $3\sigma/K$ method. To calculate the standard deviation (σ), the emission intensity of **BBCN** at 315 nm was measured ten times, and the standard deviation was calculated. Slope (K) was calculated from the fluorescence titration profile at 315 nm versus the concentration of CN^- . From these values, the LOD was found to be 189 nM (507 ppb) (Fig. S8†). The LOD was far below the maximum allowed content in drinking water (1.9 μM) set by the World Health Organization (WHO), and the results were compared with previous chemosensors for CN^- (Table S1†). Additionally, when visualized under a UV-lamp of 365 nm source, the apparent green emission of **BBCN** changed to a blue fluorescence only in the presence of cyanide ions, while the emission remained same over the addition of the anions (Fig. 2d).

The probe's ability to detect CN^- ion in the presence of other relevant competitive ions was studied. As shown in the Fig. 3a, CN^- sensing of **BBCN** is not affected by other anions despite

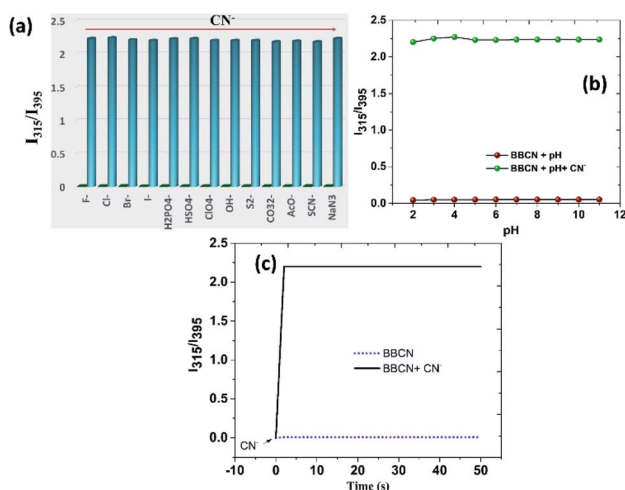


Fig. 3 (a) Fluorescent ratiometric changes of **BBCN** in the presence of the competing anions (5 equiv.) followed by the addition of CN^- (2 equiv.). (b) Effect of ratiometric fluorescence of **BBCN** in the absence and presence of CN^- as a pH function. (c) Time course of fluorescence response of the probe **BBCN** upon the addition of CN^- .

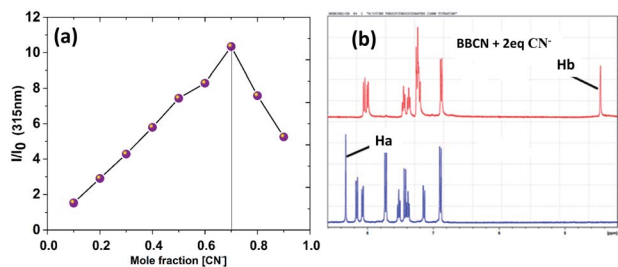


Fig. 4 (a) Job plot of probe **BBCN** and CN^- , where the intensity ratio at 315 nm was plotted against the mole fraction of CN^- . (b) ^1H NMR spectral change of **1** (2×10^{-2} M) in the absence and presence of 2 equiv. of CN^- in DMSO-d_6 .

introduction in higher equivalents and also the found fluorescence intensity is as significant as **BBCN-CN**. This competitive binding experiment clearly demonstrates the excellent selectivity of **BBCN** toward CN^- , which is due to strong nucleophilicity of CN^- . Besides, the influence of pH on the emission of the property of **BBCN** and **BBCN-CN** was studied with the range of pH solutions (2 to 11) as shown in the Fig. 3b. As the pH of the medium was adjusted between 2 and 11, the fluorescence intensity of **BBCN** and **BBCN-CN** was not affected, which indicates that **BBCN** can be used in the broader range of pH to detect CN^- of the physiological and biological samples. In general, chemosensors with short response time are highly preferred than those with delayed responses. To check the kinetics of CN^- detection by **BBCN**, the time course of fluorescence emission intensity of **BBCN** over the addition of CN^- was studied. As shown in the Fig. 3c, the fluorescence intensity ratio (I_{315}/I_{395}) reached its maximum within 1 second, indicating fluorescence response of **BBCN** towards is sensitive and rapid.

Sensing mechanism

The spectral response phenomena of probe **BBCN** to cyanide can result from CN^- nucleophilic addition of CN^- to the dicyanovinyl group as expected. This reaction process can sufficiently hinder the efficiency of the intramolecular charge transfer. The Job's plot measured using fluorescent titration method indicated that the maximum fluorescence intensity was achieved when the molar fraction of **BBCN** and CN^- was around

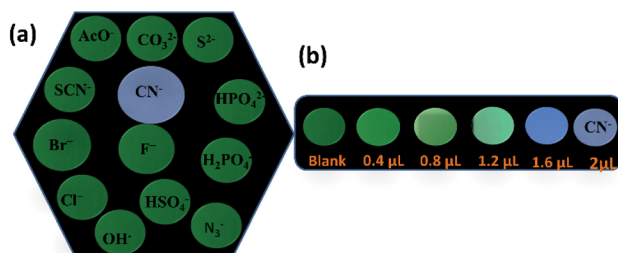


Fig. 5 (a) Color change of test strip upon dipping in a cyanide ion solution and various other anions. (b) The gradual colour change of test strip from green to blue upon dipping in cyanide ion solution of increasing concentration.



Table 1 Estimation of Fe³⁺ ion quantity in collected water samples

S. no.	Water samples ^a	CN ⁻ spiked (μM)	CN ⁻ found (μM)	Recovery (%)	R.S.D ^b (n = 3) (%)
1	Tap water	1 × 10 ⁻⁶	0.98 × 10 ⁻⁶	98	0.2
2	Lake water	1 × 10 ⁻⁶	0.92 × 10 ⁻⁶	92	1.2
3	Well water	1 × 10 ⁻⁶	0.97 × 10 ⁻⁶	97	0.23
4	Mineral water	1 × 10 ⁻⁶	0.95 × 10 ⁻⁶	95	0.3
5	Distilled water	1 × 10 ⁻⁶	0.99 × 10 ⁻⁶	99	0.19
6	Purified water	1 × 10 ⁻⁶	0.97 × 10 ⁻⁶	97	0.23

^a Water samples were collected from in and around VIT campus, Vellore. ^b Relative standard deviation conditions: 10 μM BBCN in a mixed solution of CH₃CN/water (7 : 3).

0.75, showing the 1 : 2 binding event (Fig. 4a). The sensing mechanism was further explored by recording and comparing the ¹H NMR of BBCN and BBCN + CN⁻ reaction mixture. ¹H NMR spectra of BBCN, and the resultant product is shown in the Fig. 4b. The resonance signal at δ = 8.33 ppm was ascribed to the vinylic proton (H_a). After adding an excess of CN⁻ the resonance signal corresponding to vinylic proton (H_a) at 8.33 ppm completely disappeared, while a new signal of the α-proton (H_b) appeared at 4.46 ppm, which can be attributed to dicyano ethyl proton. As a result, the aromatic proton displayed a more significant upfield shift than those probes due to the broken conjugated bridge. These observations indicated that the cyanide anion was added to the vinyl group *via* nucleophilic addition reaction. The formation of new nucleophilic addition product was further confirmed by recording ESI-MS spectra. The peak observed at *m/z* = 842.19 corresponded to BBCN + CN⁻ (Fig. S9†). The results confirmed the selective detection of CN⁻ based on nucleophilic addition of CN⁻ ion in the π-conjugated position of dicyanovinyl moiety.^{16,54–62} In addition, the structure and the binding mechanism were further analysed by FT-IR analysis of free BBCN and BBCN–CN⁻ (Fig. S10†). BBCA revealed clear and strong characteristic absorption bands for disubstituted alkene C=C bond (C=C bending, 758 cm⁻¹) and geminal C–CN bond (C–CN bending, 819 cm⁻¹). Both of these peaks completely disappeared for BBCN–CN⁻ and a new strong peak appeared in the finger print region at 952 cm⁻¹ which is due to C–C bending which corroborates well with the structure of BBCN–CN⁻.

Real-time application

Applications in test strips. To investigate the practical utility of the fluorescence probe BBCN for the selective and sensitive detection of CN⁻ ion, especially in the field of onsite pollution inspection, test strips-based detection was demonstrated. BBCN coated test strips were prepared by dipping Whatman filter paper into BBCN solution CH₃CN/HEPES in water buffer in water pH 7.2 (7 : 3 v/v) followed by drying in air. When the test strips were immersed in various anions, colour change from green to blue was observed only with CN⁻ (Fig. 5a).

Besides, to get a direct quantitative detection, test strips were dipped in different vials, increasing the cyanide ion concentration, gradual colour transformation from green to blue was observed (Fig. 5b). These observations indicate that BBCN

coated test strip could be conveniently used to detect cyanide ion for sensitive and rapid detection of cyanide ions in practical samples without using expensive equipment.

Application of BBCN in practical water analysis. Standard addition method was applied to study the useful utility of BBCN toward CN⁻ ion in real water samples collected from various water bodies from VIT campus. The collected water samples were spiked with a known concentration of cyanide ion, and recovery yields were determined based on the calibration curve. Recovery outcomes indicated reliable recovery percentages with low RSD (Table 1). With this accurate, precise and simplified method, BBCN could be a pertinent candidate for CN⁻ determination in environmental samples.

Conclusions

In summary, a new efficient BINOL based fluorescent ratio-metric sensor BBCN for the highly sensitive and selective detection of CN⁻ has been developed. BBCN undergoes remarkable hypochromic shift both in the absorbance and emission spectra occurs over the addition of CN⁻ ion as a result of ICT suppression. Spectral changes of BBCN have excellent selectivity towards CN⁻ ion with rapid response time. LOD was found to be in the range of 189 nm (507 ppb). This probe was successfully utilized to detect CN⁻ in real time water samples collected from various water bodies with satisfactory results. Moreover, BBCN based test strips can quickly and conveniently developed and for selective and sensitive detection of CN⁻.

Conflicts of interest

There are no conflicts to declare.

Acknowledgements

Sathish S and Dhanapal J thank VIT University for providing financial support through research associateship. The DST-FIST NMR facility at VIT University is duly acknowledged. The authors thank Dr R. Srinivasan, SSL-VIT for language editing.

References

- 1 R. Sakai, T. Satoh and T. Kakuchi, *Polym. Rev.*, 2017, **57**, 159–174.



- 2 R. Martínez-Mañez and F. Sancenón, *Chem. Rev.*, 2003, **103**, 4419–4476.
- 3 Y. Liu, Y. Hu, S. Lee, D. Lee and J. Yoon, *Bull. Korean Chem. Soc.*, 2016, **37**, 1661–1678.
- 4 P. Molina, F. Zapata and A. Caballero, *Chem. Rev.*, 2017, **117**, 9907–9972.
- 5 C. J. Serpell and P. D. Beer, in *Comprehensive Supramolecular Chemistry II*, ed. J. L. Atwood, Elsevier, Oxford, 2017, pp. 351–385.
- 6 Q. Lin, F. Zheng, T.-T. Lu, J. Liu, H. Li, T.-B. Wei, H. Yao and Y.-M. Zhang, *Sens. Actuators, B*, 2017, **251**, 250–255.
- 7 R. Arumugaperumal, V. Srinivasadesikan, M. V. Ramakrishnam Raju, M.-C. Lin, T. Shukla, R. Singh and H.-C. Lin, *ACS Appl. Mater. Interfaces*, 2015, **7**, 26491–26503.
- 8 M. J. Langton, Y. Xiong and P. D. Beer, *Chem.–Eur. J.*, 2015, **21**, 18910–18914.
- 9 P. A. Gale, N. Busschaert, C. J. E. Haynes, L. E. Karagiannidis and I. L. Kirby, *Chem. Soc. Rev.*, 2013, **43**, 205–241.
- 10 N. Busschaert, C. Caltagirone, W. Van Rossom and P. A. Gale, *Chem. Rev.*, 2015, **115**, 8038–8155.
- 11 A. Brown and P. D. Beer, *Chem. Commun.*, 2016, **52**, 8645–8658.
- 12 D. M. Gillen, C. S. Hawes and T. Gunnlaugsson, *J. Org. Chem.*, 2018, **83**, 10398–10408.
- 13 M. I. Rednic, R. A. Varga, A. Bende, I. G. Grosu, M. Miclăuș, N. D. Hădade, A. Terec, E. Bogdan and I. Grosu, *Chem. Commun.*, 2016, **52**, 12322–12325.
- 14 M. H. Chua, H. Zhou, T. T. Lin, J. Wu and J. Xu, *J. Mater. Chem. C*, 2017, **5**, 12194–12203.
- 15 F. Wang, L. Wang, X. Chen and J. Yoon, *Chem. Soc. Rev.*, 2014, **43**, 4312–4324.
- 16 T. M. Ebaston, G. Balamurugan and S. Velmathi, *Anal. Methods*, 2016, **8**, 6909–6915.
- 17 Y.-L. Leng, J.-H. Zhang, Q. Li, Y.-M. Zhang, Q. Lin, H. Yao and T.-B. Wei, *New J. Chem.*, 2016, **40**, 8607–8613.
- 18 Y. Zhang, D. Li, Y. Li and J. Yu, *Chem. Sci.*, 2014, **5**, 2710–2716.
- 19 X. Chen, S.-W. Nam, G.-H. Kim, N. Song, Y. Jeong, I. Shin, S. K. Kim, J. Kim, S. Park and J. Yoon, *Chem. Commun.*, 2010, **46**, 8953–8955.
- 20 B. Aydiner, Ö. Şahin, D. Çakmaz, G. Kaplan, K. Kaya, Ü. Ö. Özdemir, N. Seferoğlu and Z. Seferoğlu, *New J. Chem.*, 2020, **44**, 19155–19165.
- 21 S. Li, F. Huo, K. Ma, Y. Zhang and C. Yin, *New J. Chem.*, 2021, **45**, 1216–1220.
- 22 S. Malkondu, S. Erdemir and S. Karakurt, *Dyes Pigm.*, 2020, **174**, 108019.
- 23 A. Popczyk, Y. Cheret, A. El-Ghayoury, B. Sahraoui and J. Mysliwiec, *Dyes Pigm.*, 2020, **177**, 108300.
- 24 G. Sun, W. Chen, Y. Liu, X. Jin, Z. Zhang and J. Su, *Dyes Pigm.*, 2020, **176**, 108224.
- 25 Y.-D. Lin, Y.-S. Pen, W. Su, K.-L. Liao, Y.-S. Wen, C.-H. Tu, C.-H. Sun and T. J. Chow, *Chem.–Asian J.*, 2012, **7**, 2864–2871.
- 26 Y. Liu, J. s. Du, S. I. Qi, L. b. Zhu, Q. b. Yang, H. Xu and Y. x. Li, *Luminescence*, 2021, **36**, 336–344.
- 27 W.-J. Qu, W.-T. Li, H.-L. Zhang, T.-B. Wei, Q. Lin, H. Yao and Y.-M. Zhang, *J. Heterocycl. Chem.*, 2018, **55**, 879–887.
- 28 L. Yang, X. Li, J. Yang, Y. Qu and J. Hua, *ACS Appl. Mater. Interfaces*, 2013, **5**, 1317–1326.
- 29 L. Long, X. Yuan, S. Cao, Y. Han, W. Liu, Q. Chen, Z. Han and K. Wang, *ACS Omega*, 2019, **4**, 10784–10790.
- 30 X. Cheng, R. Tang, H. Jia, J. Feng, J. Qin and Z. Li, *ACS Appl. Mater. Interfaces*, 2012, **4**, 4387–4392.
- 31 W.-C. Lin, S.-K. Fang, J.-W. Hu, H.-Y. Tsai and K.-Y. Chen, *Anal. Chem.*, 2014, **86**, 4648–4652.
- 32 P. S. Kumar, P. R. Lakshmi and K. P. Elango, *New J. Chem.*, 2019, **43**, 675–680.
- 33 X. Sun, Y. Wang, X. Deng, J. Zhang and Z. Zhang, *RSC Adv.*, 2016, **6**, 10266–10271.
- 34 L. Hou, F. Li, J. Guo, X. Zhang, X. Kong, X. T. Cui, C. Dong, Y. Wang and S. Shuang, *J. Mater. Chem. B*, 2019, **7**, 4620–4629.
- 35 J. Kang, F. Huo, Y. Zhang, J. Chao, T. E. Glass and C. Yin, *Spectrochim. Acta, Part A*, 2019, **209**, 95–99.
- 36 Y. Hao, K. H. Nguyen, Y. Zhang, G. Zhang, S. Fan, F. Li, C. Guo, Y. Lu, X. Song, P. Qu, Y.-N. Liu and M. Xu, *Talanta*, 2018, **176**, 234–241.
- 37 L. Lan, T. Li, T. Wei, H. Pang, T. Sun, E. Wang, H. Liu and Q. Niu, *Spectrochim. Acta, Part A*, 2018, **193**, 289–296.
- 38 W.-C. Lin, J.-W. Hu and K.-Y. Chen, *Anal. Chim. Acta*, 2015, **893**, 91–100.
- 39 G.-L. Fu and C.-H. Zhao, *Tetrahedron*, 2013, **69**, 1700–1704.
- 40 A. S. Gupta, K. Paul and V. Luxami, *Inorg. Chim. Acta*, 2016, **443**, 57–63.
- 41 X. Feng, Y. Wang, W. Feng and Y. Peng, *Chin. Chem. Lett.*, 2020, **31**, 2960–2964.
- 42 K. Velmurugan and R. Nandhakumar, *J. Lumin.*, 2015, **162**, 8–13.
- 43 C. Monterde, R. Navarro, M. Iglesias and F. Sánchez, *J. Catal.*, 2019, **377**, 609–618.
- 44 S. Munusamy and S. Kulathu Iyer, *Tetrahedron: Asymmetry*, 2016, **27**, 492–497.
- 45 S. Munusamy, V. P. Muralidharan and S. K. Iyer, *Sens. Actuators, B*, 2017, **250**, 244–249.
- 46 S. K. Munusamy, K. Thirumoorthy, V. P. Muralidharan, U. Balijapalli and S. K. Iyer, *Sens. Actuators, B*, 2017, **244**, 175–181.
- 47 L. Pu, *Acc. Chem. Res.*, 2012, **45**, 150–163.
- 48 M.-Q. Wang, K. Li, J.-T. Hou, M.-Y. Wu, Z. Huang and X.-Q. Yu, *J. Org. Chem.*, 2012, **77**, 8350–8354.
- 49 X. Liu, X. Yang, Y. Fu, C. Zhu and Y. Cheng, *Tetrahedron*, 2011, **67**, 3181–3186.
- 50 M. Dong, Y.-M. Dong, T.-H. Ma, Y.-W. Wang and Y. Peng, *Inorg. Chim. Acta*, 2012, **381**, 137–142.
- 51 C. Fan, X. Huang, L. Han, Z. Lu, Z. Wang and Y. Yi, *Sens. Actuators, B*, 2016, **224**, 592–599.
- 52 J. Li, C. Yin, F. Huo, K. Xiong, J. Chao and Y. Zhang, *Sens. Actuators, B*, 2016, **231**, 547–551.
- 53 F. Li, G. Wei, Y. Sheng, Y. Quan, Y. Cheng and C. Zhu, *Polymer*, 2014, **55**, 5689–5694.
- 54 E. Thanayupong, K. Suttisintong, M. Sukwattanasinitt and N. Niamnont, *New J. Chem.*, 2017, **41**, 4058–4064.



- 55 Q. Zou, X. Li, Q. Xu, H. Ågren, W. Zhao and Y. Qu, *RSC Adv.*, 2014, **4**, 59809–59816.
- 56 H. Li, X. Wu, Y. Xu, H. Tong and L. Wang, *Polym. Chem.*, 2014, **5**, 5949–5956.
- 57 R. K. Konidena and K. R. J. Thomas, *RSC Adv.*, 2014, **4**, 22902–22910.
- 58 W. Chen, Z. Zhang, X. Li, H. Ågren and J. Su, *RSC Adv.*, 2015, **5**, 12191–12201.
- 59 E. Jeong, S. Yoon, H. S. Lee, A. Kumar and P. S. Chae, *Dyes Pigm.*, 2019, **162**, 348–357.
- 60 A. Tigreros, J.-C. Castillo and J. Portilla, *Talanta*, 2020, **215**, 120905.
- 61 A. Ozdemir and S. Erdemir, *J. Photochem. Photobiol. Chem.*, 2020, **390**, 112328.
- 62 E. Ramachandran, S. A. A. Vandarkuzhali, G. Sivaraman and R. Dhamodharan, *Chem.–Eur. J.*, 2018, **24**, 11042–11050.

